



PRIFYSGOL  
**BANGOR**  
UNIVERSITY

## Meta-Mass Shift Chemical (MeMSSChem) profiling of metabolomes from coral reefs

Hartmann, Aaron; Petras, Daniel; Quinn, Robert; Protsyuk, Ivan; Archer, Frederick; Ransome, Emma; Williams, Gareth; Bailey, Barbara; Vermeij, Mark; Alexandrov, Theodore; Dorrestein, Pieter; Rohwer, Forest

**Proceedings of the National Academy of Sciences of the United States of America**

DOI:

[10.1073/pnas.1710248114](https://doi.org/10.1073/pnas.1710248114)

Published: 31/10/2017

Peer reviewed version

[Cyswllt i'r cyhoeddiad / Link to publication](#)

*Dyfyniad o'r fersiwn a gyhoeddwyd / Citation for published version (APA):*

Hartmann, A., Petras, D., Quinn, R., Protsyuk, I., Archer, F., Ransome, E., Williams, G., Bailey, B., Vermeij, M., Alexandrov, T., Dorrestein, P., & Rohwer, F. (2017). Meta-Mass Shift Chemical (MeMSSChem) profiling of metabolomes from coral reefs. *Proceedings of the National Academy of Sciences of the United States of America*, 114(44), 11685-11690. <https://doi.org/10.1073/pnas.1710248114>

### Hawliau Cyffredinol / General rights

Copyright and moral rights for the publications made accessible in the public portal are retained by the authors and/or other copyright owners and it is a condition of accessing publications that users recognise and abide by the legal requirements associated with these rights.

- Users may download and print one copy of any publication from the public portal for the purpose of private study or research.
- You may not further distribute the material or use it for any profit-making activity or commercial gain
- You may freely distribute the URL identifying the publication in the public portal ?

### Take down policy

If you believe that this document breaches copyright please contact us providing details, and we will remove access to the work immediately and investigate your claim.

# Meta-Mass Shift Chemical (MeMSChem) profiling of metabolomes from coral reefs

Aaron C. Hartmann<sup>1,2,\*</sup>, Daniel Petras<sup>3</sup>, Robert A. Quinn<sup>3</sup>, Ivan Protsyuk<sup>4</sup>, Frederick I. Archer<sup>5</sup>, Emma J. Ransome<sup>2</sup>, Gareth J. Williams<sup>6</sup>, Barbara A. Bailey<sup>7</sup>, Mark J. A. Vermeij<sup>8,9</sup>, Theodore Alexandrov<sup>3,4</sup>, Pieter C. Dorrestein<sup>3</sup>, Forest L. Rohwer<sup>1</sup>

## Affiliations

<sup>1</sup> Department of Biology, San Diego State University, San Diego, CA

<sup>2</sup> National Museum of Natural History, Smithsonian Institution, Washington, D.C.

<sup>3</sup> Collaborative Mass Spectrometry Innovation Center, Skaggs School of Pharmacy and Pharmaceutical Science, University of California San Diego, La Jolla, CA

<sup>4</sup> Structural and Computational Biology Unit, European Molecular Biology Laboratory, Heidelberg, Germany

<sup>5</sup> National Oceanic and Atmospheric Administration, Southwest Fisheries Science Center, La Jolla, CA

<sup>6</sup> School of Ocean Sciences, Bangor University, LL59 5AB, UK

<sup>7</sup> Department of Mathematics and Statistics, San Diego State University, San Diego, CA

<sup>8</sup> Carmabi Foundation, Piscaderabaai, Willemstad, Curaçao

<sup>9</sup> Aquatic Microbiology, Institute for Biodiversity and Ecosystem Dynamics (IBED) University of Amsterdam, Amsterdam, the Netherlands

## \*Corresponding author:

Department of Invertebrate Zoology

MRC 163 PO BOX 37012

National Museum of Natural History

10<sup>th</sup> Street and Constitution Avenue NW

Washington DC 20013-7012

aaron.hartmann@gmail.com

+1.802.279.8109

**Short title:** Meta-Mass Shift Chemical profiling

**Classification:** Biological Sciences/Biochemistry

**Keywords:** untargeted metabolomics, molecular networking, small molecules, coral reefs

42 **Abstract**

43 Untargeted metabolomics of environmental samples routinely detects thousands  
44 of small molecules, the vast majority of which cannot be identified. Meta-Mass  
45 Shift Chemical (MeMSChem) profiling was developed to identify mass  
46 differences between related molecules using metabolomic networks. This  
47 approach illuminates metabolome-wide relationships between molecules and the  
48 putative chemical groups that differentiate them (e.g., H<sub>2</sub>, CH<sub>2</sub>, COCH<sub>2</sub>).  
49 MeMSChem was used to analyze a publicly-available metabolomic dataset of  
50 coral, algal, and fungal mat holobionts (i.e., the host and its associated microbes  
51 and viruses) sampled from some of Earth's most remote and pristine coral reefs.  
52 Each type of holobiont had unique mass shift profiles, even when the analysis  
53 was restricted to parent molecules found in all samples. This result suggests that  
54 holobionts modify the same molecules in different ways and offers insights into  
55 the generation of molecular diversity. Three genera of stony corals had distinct  
56 patterns of molecular relatedness despite their high degree of taxonomic  
57 relatedness. MeMSChem profiles also partially differentiated between individuals,  
58 suggesting that every coral reef holobiont is a potential source of novel chemical  
59 diversity.

60

61 **Significance Statement**

62 Coral reef taxa produce a diverse array of molecules, some of which are  
63 important pharmaceuticals. To better understand how molecular diversity is

64 generated on coral reefs, metabolomes were analyzed using a novel approach  
65 called Meta-Mass Shift Chemical (MeMSChem) profiling. MeMSChem uses the  
66 mass differences between molecules in networks to determine how molecules  
67 are related. Interestingly, the same molecules gain and lose chemical groups in  
68 different ways depending on the taxa it came from, offering a partial explanation  
69 for high molecular diversity on coral reefs.

70 \body

71 Untargeted tandem mass spectrometry is a powerful tool for wide-scale  
72 analysis of small molecules. The resulting metabolomes are potential treasure  
73 troves of new molecules and chemistries, but a major problem in realizing this  
74 potential is that most detected molecules cannot be identified (1-5). One possible  
75 solution is to use spectral fragmentation similarity to identify relatives of known  
76 molecules to generate novel annotations (6-8). These approaches have rapidly  
77 expanded reference databases, but they remain inherently limited by the number  
78 of known molecules. Therefore, there is a need for analyses that do not rely upon  
79 molecular reference libraries (9).

80 The online platform Global Natural Products Social Molecular Networking  
81 (GNPS; 5) uses spectral fragmentation patterns to compare tens of thousands of  
82 molecular features and create networks of structurally-similar molecules. Here  
83 we expand the analysis of GNPS networks to identify chemical differences  
84 between related molecules (Figure 1). This approach is called Meta-Mass Shift  
85 Chemical (MeMSChem) profiling and it uses the mass differences (or mass  
86 shifts) between related molecules to identify and annotate known chemical  
87 groups such as H<sub>2</sub>, CH<sub>2</sub>, COCH<sub>2</sub>, etc. Annotating molecules based on their mass  
88 shifts facilitates correlations between metabolomics, biochemistry and genomics,  
89 which could help pinpoint sites of molecular modifications resulting from known  
90 and unknown enzymatic activities.

91 Coral reefs are noted sources of novel, commercially-useful compounds  
92 (10). Reef holobionts (e.g., corals, sponges, and algae with their associated viral  
93 and microbial communities; 11) have unique metabolomes, with a high degree of  
94 within-holobiont similarity (12, 13). The positive relationship between taxonomic  
95 and molecular diversity is evident at the ecosystem level, but mechanisms  
96 explaining how high molecular diversity is generated remain missing. To address  
97 this question, MeMSChem was applied to an existing dataset (12) comprised of  
98 seven coral reef holobiont types collected in the Line Islands, which are some of  
99 the most remote and pristine coral reefs in the world (14, 15). MeMSChem  
100 profiling showed that molecular mass shift patterns differ significantly between  
101 holobionts, offering new insights into why high molecular diversity is found on  
102 coral reefs.

103

## 104 **Results**

105 *Identifying redundant mass shifts in metabolomes in coral reef holobionts:*

106 The dataset used as the basis for creating MeMSChem was previously published  
107 in Quinn et al. 2016 (12) and can be found on the Mass spectrometry Interactive  
108 Virtual Environment (MassIVE) at <https://massive.ucsd.edu/> with the accession  
109 number: MSV000078598. This dataset was derived from an LC-MS/MS analysis  
110 of three genera of scleractinian coral (*Montipora* spp., *Pocillopora* spp., *Porites*  
111 spp.), two coralline algae (crustose coralline algae [CCA] and *Halimeda* sp.), two  
112 non-calcifying algae (macroalgae and turf algae) and a fungal mat.

113 The online platform Global Natural Products Social Molecular Networking  
114 (GNPS, gnps.ucsd.edu; Figure S1; 5) was used to cluster identical MS/MS  
115 spectra into nodes and identify the degree to which each node was structurally  
116 similar (i.e., related) to other nodes (henceforth referred to as molecular features)  
117 based on a cosine score of spectral similarity. All pairs of molecular features  
118 receiving a cosine score above a threshold of 0.6 were considered to be related  
119 and connected in the network (see SI Materials and Methods for more details  
120 regarding the cosine score threshold). Each mass shift between network  
121 connections was then mined for multiple (i.e., redundant) occurrences (Figure  
122 1B). When five or more molecular feature pairs differed by a mass of  $m/z \pm$   
123 0.001, the mass shift was counted. All molecular features comprising the pairs  
124 with this mass shift were assigned to a bin (Figure 1C-E, see the SI Materials  
125 and Methods for more details).

126 MeMSChem profiling identified 62 mass shifts that passed the filter of  $m/z$   
127  $\pm 0.001$  and greater than 5 occurrences (Table S1). Among these mass shifts, 10  
128 were annotated to known adducts and artifacts and were removed prior to further  
129 analyses (Table S1 and S2). The remaining mass shifts were annotated to  
130 known chemical groups involving hydrogen, carbon, and oxygen where possible,  
131 leading to the annotation of 13 of the 62 mass shifts identified (Table S1). This  
132 represents a conservative list of annotations and the additional mass shifts  
133 identified here may be annotatable in future investigations.

134 Mass shifts of 0 were abundant in the networks and may represent  
135 isomers. These mass shifts were removed due to the likelihood that two isomers  
136 were merged into a single molecular feature or that the same molecular feature  
137 was split into two molecules during networking, due to the high degree or  
138 spectral similarity or differences in the number of observable fragments,  
139 respectively. An approach using retention time differences or chiral separation  
140 columns should be employed to separate isomers in future applications of  
141 MeMSChem.

142 *Quantifying mass shifts in holobionts: MS/MS-based molecular features*  
143 associated with the redundant mass shifts were quantified from the MS scan of  
144 the parent molecule using the Optimus software  
145 (<https://github.com/MolecularCartography/Optimus>; Figure 1C). A molecular  
146 feature filter was applied to remove features that were not detected in all  
147 samples. Consequently, only the features present in all samples were quantified.  
148 This filter allowed us to determine whether holobionts exhibit different mass shifts  
149 associated with the same molecules (c.f., different mass shifts associated with  
150 molecules that are only found that holobiont; Figure 1E-F).

151 Three forms of metabolome-wide data were generated for each sample  
152 (Figure 1A-C). First, all instances where a redundant mass shift was observed in  
153 the network was tabulated for each sample. These 'counts' data provided a  
154 metric of the commonness and rarity of each mass shift in each sample (Figure  
155 1D). Second, the abundance of every molecular feature was summed by mass



156 shift regardless of whether that feature was the higher or lower mass feature in a  
157 network pair. These 'summed abundance' data provided a metric for the overall  
158 occurrence of each mass shift throughout each sample (Figure 1E; see the SI  
159 Materials and Methods for equations). Third, for each network pair, the difference  
160 in abundance between the more and less massive feature was calculated, then  
161 these values were summed by mass shift for each sample (Figure 1F, see the SI  
162 Materials and Methods for equations). These 'difference in abundance' data  
163 reflected whether, metabolome-wide, molecules were more likely to gain or lose  
164 a given mass, potentially reflecting active interconversion or branching of largely  
165 shared biosynthetic pathways. All resultant data are provided in the Supporting  
166 Information 'Processed Data' file. Among the redundant mass shifts, seven of the  
167 ten most redundant mass shifts were putatively annotated to known chemical  
168 groups, constituting nearly 50% of the network pairs isolated from the networks.  
169 These mass shifts included  $m/z$  2.016, 14.016, 28.032, 56.064, 26.016, 18.010,  
170 12.000, which were putatively annotated as H<sub>2</sub>, CH<sub>2</sub>, C<sub>2</sub>H<sub>4</sub>, C<sub>4</sub>H<sub>8</sub>, C<sub>2</sub>H<sub>2</sub>, H<sub>2</sub>O, and  
171 C, respectively.

172 *Examining known mass shifts associated with library-identified molecular*  
173 *features:* Instances in which known mass shifts were associated with identified  
174 molecules provided conformational evidence that mass shifts were correctly  
175 annotated. Four examples are highlighted in Figure 2B: 1) A feature identified as  
176 phenatro-furanone with a mass shift of  $m/z$  18.014 (H<sub>2</sub>O; Figure 2B Example 1;  
177 Figure S2). 2) A subnetwork with three forms of Lyso-PAF and related

178 compounds (Figure 2B Example 2; Figure S3). The identification of one  
179 molecular feature, Lyso-PAF C-16, in these sample was previously confirmed  
180 using a reference standard by Quinn et al. 2016 (12). This subnetwork is  
181 particularly informative because the three identified compounds were networked  
182 to one another, showing that the mass shifts truly correspond to a de-saturation  
183 and elongation of a fatty acid chain,  $m/z$  2.018 ( $H_2$ ) and  $m/z$  28.032 ( $C_2H_4$ ). 3) A  
184 subnetwork of ceramide-related compounds (Figure 2B Example 3; Figure S4)  
185 with mass shifts of  $m/z$  2.015 ( $H_2$ ),  $m/z$  14.015 ( $CH_2$ ), and 165.057 ( $C_6H_{10}O_5$ ,  
186 glycosylation). A coral-associated ceramide was recently identified (16) with one  
187 additional desaturation relative to the ceramide identified here, and this newly-  
188 identified ceramide has an extremely similar mass ( $m/z$  536.504) to the unknown  
189 feature ( $m/z$  536.508) networked to the ceramide here. The newly-identified  
190 ceramide also differs in mass from the identified ceramide by  $m/z$  2.015,  
191 consistent with one fewer saturation. 4) A subnetwork of three unidentified  
192 molecules with mass shifts of  $m/z$  28.032 ( $C_2H_4$ ),  $m/z$  28.033 ( $C_2H_4$ ), and  $m/z$   
193 56.065 ( $C_4H_8$ ; Figure S5).

194 *Differences in mass shift profiles between types of holobionts:* To  
195 determine how well MeMSChem profiling resolved each holobiont type, Random  
196 Forests classification (17) was used to generate an out-of-bag error (henceforth  
197 referred to as 'model error'), which reflects the extent to which the model  
198 correctly categorized every sample (i.e., whether *Halimeda* sp. samples were  
199 correctly placed into the model's *Halimeda* group). Random Forests offers

200 exceptional classification performance and is robust to non-normally distributed  
201 data and correlated predictors (18), both of which were present in this dataset  
202 (see the Supporting Information 'Processed Data' file).

203         The usefulness of re-categorizing molecules by their mass shifts was first  
204 evaluated based on the number of times that each mass shift was observed  
205 (counts data described above). The model error of the Random Forests  
206 classifying holobiont types using the counts data was 0.44, which indicates that  
207 44% of the time samples were assigned to the incorrect holobiont type. The  
208 resolution gained from the observed counts data (i.e., actual data) was compared  
209 to that from 1000 permutations of the data in which pairs were randomly binned  
210 and counted while keeping the original proportions consistent. The observed  
211 counts data outperformed 95% of the randomly-generated datasets, suggesting  
212 that the counts of redundant mass shifts aided in differentiating between  
213 holobiont types despite the relatively high model error (Figure 3A).

214         Molecular abundance data were then incorporated into the analysis and  
215 compared against the holobiont resolution gained from the counts data. When  
216 the summed abundances of each mass shift among molecules present in all  
217 holobionts were considered, the model error from the abundance data was 0.36  
218 (Figure 3B). Therefore, incorporating feature abundance data improved the  
219 accuracy of the model by 8% when resolving between holobiont types. The value  
220 of summing feature abundances by mass shift was also tested by comparing its  
221 accuracy to the models of 1000 permutations of the data in which network pairs

222 were randomly binned and summed while keeping the original proportions  
223 consistent (as was done for the counts data above). Among only the molecular  
224 features present in all holobionts, summing of feature abundances by mass shift  
225 resolved holobiont types better than 90% of the datasets generated from random  
226 summing of feature abundances (Figure 3B). Thus, binning abundance data by  
227 redundant mass shifts categorizes molecules in a non-random manner.  
228 Molecular abundances binned by mass shifts also reflected differences among  
229 holobiont types better than when holobionts were compared with data that lacks  
230 any feature abundance information (i.e., counts of the number of mass shifts).

231         To determine whether mass shifts may reflect active sites of molecular  
232 interconversions, as would be expected if a molecular modification had occurred,  
233 the summed abundances were compared to the differences in abundance  
234 between molecular pairs by mass shift. This is akin to one molecule being the  
235 reactant and the other the product. The model error of the difference in  
236 abundance data was 0.34, demonstrating that organizing the data by the  
237 differences in abundances slightly outperformed the summed abundance data  
238 (model error = 34% and 36%, respectively; Figure 3C). When compared to 1000  
239 random permutations of the actual data, the difference in abundance data  
240 outperformed 86% of the random models.

241         Classification was further improved by incorporating the full molecular  
242 dataset, and thus the molecules that were present in all holobionts and the  
243 molecules that were only found in one or a few holobionts. When these

244 molecules were included, the model error was 0.02. This reflects a 32%  
245 decrease in the model error relative to when only molecules found in all  
246 holobionts were considered and was nearly perfect in assigning samples to their  
247 correct holobiont type. The real data outperformed 92% of randomly generated  
248 datasets (Figure 3D and summarized in Figure 3E). These results suggest that  
249 the highest level of holobiont resolution is achieved when: 1) molecular features  
250 were binned by the redundant mass shifts they exhibit, 2) molecular abundances  
251 were included as the difference in abundance between molecules in a network  
252 pair, and 3) molecules/pairs that are only found in certain holobionts were  
253 included in addition to those molecules present in all holobionts.

254 *Mass shifts that best distinguish each holobiont type:* Among the  
255 molecular features present in all holobionts, coral genera were best differentiated  
256 from one another by mass shifts corresponding to two carbons that were either  
257 saturated ( $m/z$  28.032,  $C_2H_4$  or  $2*CH_2$ ) or unsaturated ( $m/z$  26.016  $C_2H_2$ ;  $p < 0.01$   
258 for both; Figure 4A). The three coral genera exhibited distinct patterns between  
259 these two mass shifts: molecular features of *Montipora* exhibited the addition of  
260  $C_2H_4$  and loss of  $C_2H_2$ , while *Pocillopora* exhibited the opposite pattern. *Porites*-  
261 associated molecules did not gain or lose either mass shift. Putative  $CH_2$  and  
262  $CH_2OOH$  mass shifts best differentiated the non-coral holobionts ( $p < 0.01$  for  
263 both; Figure 4B). *Halimeda* features predominantly gained  $CH_2$ , as did turf algae,  
264 the fungal mat, and all of the corals, though to a lesser degree than *Halimeda*.  
265 Additions of  $CH_2OOH$  were unique to *Halimeda*. Corals were best differentiated

266 from non-corals based on larger losses of CO and H<sub>2</sub>, the latter suggesting a  
267 dehydrogenated state perhaps due to higher concentrations of unsaturated lipids.

268

## 269 **Discussion**

270 MeMSChem profiling provides an approach to identify mass shifts  
271 between related molecules and assign them to known chemical groups in  
272 complex metabolomes. Seven coral reef holobiont types were well resolved by  
273 MeMSChem profiling. Even among molecular features detected in all holobionts,  
274 mass shift profiles differed among holobiont types, suggesting that each type of  
275 holobiont is modifying the same molecules in different ways. The chemical  
276 differences between holobionts was much more apparent when all molecules  
277 were considered (i.e., molecules only produced by certain holobionts were also  
278 incorporated), suggesting that disparate mass shift patterns play a role in  
279 generating molecular diversity in this ecosystem. Shifts in the abundance of  
280 molecules exhibiting each mass shift better resolved holobiont types than the  
281 number of times each mass shift was detected. Together, these findings suggest  
282 that holobionts differ more in their patterns of molecular abundance changes  
283 (akin to gene expression) than in the diversity of mass shifts they can carry out  
284 (akin to genomic diversity).

285 *Mass shifts associated with holobionts reflect differences in molecular*  
286 *diversity:* By focusing on the differences in mass shift profiles between related  
287 molecules, MeMSChem profiling expands metabolomic analysis beyond

288 molecular matches in reference libraries to systemic insights into holobiont  
289 biochemistry. If annotated mass shifts reflect single types or classes of molecular  
290 modifications catalyzed by enzymes, then disparate mass shift patterns among  
291 holobionts may arise for multiple reasons. Holobionts for which the hosts have  
292 large genomic differences, such as stony corals and turf algae, may merely  
293 possess different biochemical pathways. Among closely-related holobiont types  
294 such as the three stony coral genera, the distinct patterns of molecular  
295 relatedness may arise from differential expression of shared genes. Yet, the  
296 largest disparity among coral holobionts was found by including the mass shifts  
297 of molecules that are unique to each holobiont. This suggests that the mass  
298 shifts of holobiont-specific molecules largely generate each coral holobiont's  
299 unique biochemical profile despite the high degree of taxonomic relatedness  
300 among these corals.

301         The mass shifts that differed among holobiont types included differences  
302 putatively assigned to single and double-bonded carbon and oxygen, likely  
303 among phospholipids and their derivatives based upon the molecules identified in  
304 this dataset previously (12) and in the current analyses. These data show the  
305 expected lower saturation state of corals relative to algae (19,20) based on the  
306 mass shift of  $m/z$  2.016 putatively assigned to  $H_2$ . Greater fatty acid saturation  
307 flexibility can mitigate the damage of elevated temperatures that lead to  
308 bleaching in corals (21), suggesting that corals benefit from a higher degree of  
309 saturation flexibility and homeoviscous adaptation potential relative to the non-

310 corals studied here. While desaturations in coral molecules generate double-  
311 bonds between carbons, the shift towards gaining H<sub>2</sub>O in coral samples suggest  
312 these double bonds may be replaced by hydroxyl groups, either directly or  
313 through shifts in the relative abundances of molecules. Hydration of  
314 phospholipids can lead to conformational changes that alter membrane surface  
315 potential and signaling activity (22), suggesting that the higher abundance of  
316 hydroxyl groups in corals reflects systemic changes in cell-cell interactions and  
317 cellular signaling pathways.

318 *Applications of MeMSChem profiling:* MeMSChem offers a new way to  
319 analyze existing LC-MS/MS datasets and provides a novel approach for  
320 identifying system-wide changes in small molecules across metabolomes. Here  
321 we analyzed a dataset collected from one of the most remote places in the world.  
322 Like this dataset, other researchers may have LC-MS/MS datasets that cannot  
323 be re-sampled or recreated. Therefore, offering a way to gain novel information *in*  
324 *silico* is an attractive proposition for many working with untargeted metabolomic  
325 data.

326 While MeMSChem was applied here to uncover similarities and  
327 differences among types of holobionts, it opens doors to answering many more  
328 questions. Rather than comparing known groups, MeMSChem may be used to  
329 uncover clusters in seemingly homogenous populations (e.g., individuals of a  
330 coral species in a common environment, human patients suffering from the same  
331 disease, cohorts of offspring growing in a shared location). Annotated mass shifts



332 can also be searched for and quantified, which may be particularly useful when  
333 looking for a ubiquitous process such as antioxidant activity.

334 If molecules of interest are identified, the mass shifts around them may be  
335 used to detect putative sites of known modifications or novel biochemistries.  
336 Annotated and unknown mass shifts will require further verification with targeted  
337 analyses, such as spiking samples with authentic standards, networking, and  
338 examining the mass shifts associated with these standards. Once putative  
339 modifications are identified, genetics and molecular biology approaches can be  
340 used to confirm or identify the responsible enzyme(s). Such an approach may be  
341 particularly useful for tracking molecular changes in time-series samples, a  
342 primary need for clinicians (23). Future applications of MeMSChem may also  
343 employ a more precise binning approach, taking into account the smaller relative  
344 variance at higher masses, changes in MS accuracy across parent masses, and  
345 precursor differences. Through this process, the continued application of  
346 MeMSChem and the novel form of data it generates will produce a wealth of  
347 information from data-rich untargeted metabolomics datasets.

348 *Conclusions:* Untargeted metabolomics continues to grow as a tool to  
349 examine the complex physiologies of life on Earth. We applied an approach that  
350 analyzes untargeted metabolomic data in a new way, based on the chemical  
351 relationships between molecules. An analysis of seven coral reef holobionts  
352 demonstrated that the relationships between molecules are diverse and distinct  
353 between holobiont types. That different types of holobionts had unique

354 MeMSSchem profiles despite high genomic similarity suggests that each  
355 possesses physiological capabilities that are not easily identified through  
356 traditional genomic approaches. The distinct molecular repertoires identified in  
357 each holobiont, coupled with the wide diversity of holobiont types on coral reefs,  
358 offers new insights into why this ecosystem is an abundant source of chemical  
359 diversity.

360

## 361 **Materials and Methods**

362 *LC-MS/MS data collection and molecular networking:* Samples of seven  
363 types of holobionts (hosts and associated viral and microbial communities)  
364 including corals, algae, and a fungal mat were extracted in 70% methanol and  
365 analyzed with LC-MS/MS (as described in Quinn et al. 2016 [12]; see the SI  
366 Materials and Methods for data acquisition details). Files were submitted for  
367 molecular network analysis using the online workflow in GNPS (Figure S1; 5),  
368 which compares spectral fragmentation patterns and networks related molecules  
369 (Fig. S1). Molecular spectra were also compared against reference libraries of  
370 known molecules in GNPS. Details of the networking parameters can be found in  
371 the SI Materials and Methods.

372 *Identifying aggregations of mass shifts in network pairs:* Across all pairs,  
373 the difference in mass between each pair of networked molecular features  
374 (referred to as 'network pair mass shifts') was searched for aggregations around  
375 precise masses. Criteria for identifying aggregations (i.e., redundancies) were

376 established using the similar masses of CO and C<sub>2</sub>H<sub>4</sub> (*m/z* 27.995 and *m/z*  
377 28.031, respectively; Figure S6; see the SI Materials and Methods for details).  
378 The network pairs involved in aggregations were binned by mass shift and  
379 counted per sample ('Counts' dataset in the SI 'Processed Data' file). All  
380 molecular features involved in redundant mass shifts were then quantified using  
381 the Optimus workflow (<https://github.com/MolecularCartography/Optimus>).  
382 Optimus was used to quantify features involved in redundant mass shifts that  
383 were present in all files/holobionts, features involved in redundant mass shifts  
384 that were present in each holobiont type, and all molecular features including  
385 those that were not involved in redundant mass shifts (for normalization of the  
386 two former datasets). Molecular abundance data were then used to quantify the  
387 molecules exhibiting each mass shift and to quantify the prevailing direction of  
388 each mass shift (gaining or losing) in each sample (see the Results and SI  
389 Materials and Methods for more details).

390 *Data analysis using Random Forests:* MeMSChem data were analyzed  
391 using the ensemble machine learning algorithm Random Forests (16). The seven  
392 holobiont types were used as classifiers and MeMSChem data were used as  
393 predictors. The out-of-bag error (referred to as 'model error') indicated how well  
394 each holobiont type was resolved by the Random Forests model. Permutation  
395 tests were used to determine how well the MeMSChem data differentiated the  
396 seven holobiont types. These tests were carried out by comparing the model  
397 error of the actual data to a distribution of model errors generated from 1000

398 randomizations of the data (see the SI Materials and Methods for more details).  
399 The relative importance of each mass shift in differentiating between holobiont  
400 types was determined using the Random Forests mean decrease accuracy score  
401 and feature importance score (for each holobiont type).

402 **Supporting Information**

403 Figures S1 –S6, Table S1 –S2, SI Materials and Methods, R code for the  
404 Random Forests permutation test, and the processed data for the four datasets  
405 represented in Figure 3 can be found in the Supporting Information.

406

407 **Author Contributions**

408 A.H. developed the method, analyzed data, prepared figures, and wrote the  
409 manuscript, D.P. analyzed data and prepared figures, R.Q. analyzed data, I.P.  
410 analyzed data and contributed analytical tools, F.A. analyzed data and  
411 contributed coding and statistical approaches, E.R. analyzed data, G.W. and B.B.  
412 contributed statistical approaches, M.V. collected samples, T.A contributed tools  
413 for the mass spectrometry analysis, P.D. contributed tools for the mass  
414 spectrometry analysis and interpretation, F.R. developed the method. All authors  
415 discussed the results and commented on the manuscript.

416

417 **Competing Financial Interests**

418 The authors declare no competing financial interests.

419

420 **Acknowledgements**

421 This work was supported by NSF Partnerships for International Research and  
422 Education (PIRE) Grant (124351; F.L.R.) and the Gordon and Betty Moore  
423 Foundation (GBMF-3781; F.L.R.). This work was also supported by the NIH

424 through the grant P41 GM103484 and the NIH grant on reuse of metabolomics  
425 data R03 CA211211. European Union's Horizon 2020 Research and Innovation  
426 Programme further supported this work under grant agreement № 634402 (to TA  
427 and IP). We thank the Deutsche Forschungsgemeinschaft for supporting this  
428 work with a postdoctoral research fellowship to D.P. with grant number PE  
429 2600/1-1.  
430

431 **Literature Cited**

- 432 1. Nicholson JK, Lindon JC (2008) Systems biology: metabonomics.  
433 *Nature* 455(7216):1054-1056.
- 434 2. Cho K, Mahieu NG, Johnson SL, Patti GJ (2014) After the feature  
435 presentation: technologies bridging untargeted metabolomics and  
436 biology. *Curr Opin Biotechnol* 28:143-148.
- 437 3. da Silva RR, Dorrestein PC, Quinn RA (2015) Illuminating the dark  
438 matter in metabolomics. *Proc Natl Acad Sci* 112:12549-12550.
- 439 4. Pirhaji L, et al. (2016) Revealing disease-associated pathways by  
440 network integration of untargeted metabolomics. *Nature Methods*  
441 13:770-776.
- 442 5. Wang MX, et al. (2016) Sharing and community curation of mass  
443 spectrometry data with Global Natural Products Social Molecular  
444 Networking. *Nature Biotechnol* 34:828-837.
- 445 6. Heinonen M, Shen HB, Zamboni N, Rousu J (2012) Metabolite  
446 identification and molecular fingerprint prediction through machine  
447 learning. *Bioinformatics* 28:2333-2341.
- 448 7. Allen F, Greiner R, Wishart D (2015) Competitive fragmentation  
449 modeling of ESI-MS/MS spectra for putative metabolite identification.  
450 *Metabolomics* 11:98-110.

- 451 8. Duhrkop K, Shen HB, Meusel M, Rousu J, Bocker S (2015) Searching  
452 molecular structure databases with tandem mass spectra using  
453 CSI:FingerID. *Proc Natl Acad Sci* 112:12580-12585.
- 454 9. Van der Hooft JJJ, Wandy J, Barrett MP, Burgess KE, Rogers S (2016)  
455 Topic modeling for untargeted modification exploration in  
456 metabolomics. *Proc Natl Acad Sci* 113:13738–13743.
- 457 10. Simmons TL, et al. (2008) Biosynthetic origin of natural products  
458 isolated from marine microorganism–invertebrate assemblages. *Proc*  
459 *Natl Acad Sci* 105(12):4587-4594.
- 460 11. Rohwer F, Seguritan V, Azam F, Knowlton N (2002) Diversity and  
461 distribution of coral-associated bacteria. *Mar Ecol Prog Ser* 243:1-10.
- 462 12. Quinn RA, et al. (2016) Metabolomics of reef benthic interactions  
463 reveals a bioactive lipid involved in coral defence. *Proc R Soc Lond*  
464 283: 20160469.
- 465 13. Pye CR, Bertin MJ, Lokey RS, Gerwick WH, Linington RG (2017)  
466 Retrospective analysis of natural products provides insights for future  
467 discovery trends. *Proc Natl Acad Sci* 114(22): 5601-5606.
- 468 14. Dinsdale EA, et al. (2008) Microbial ecology of four coral atolls in the  
469 Northern Line Islands. *PloS one* 3:e1584.
- 470 15. Smith JE, et al. (2016). Re-evaluating the health of coral reef  
471 communities: baselines and evidence for human impacts across the  
472 central Pacific. *Proc R Soc B* 283: 20151985.



- 473 16. Eltahawy NA, et al. (2015) Mechanism of action of antiepileptic  
474 ceramide from Red Sea soft coral *Sarcophyton auritum*. *Bioorg Med*  
475 *Chem Lett* 25(24):5819-5824.
- 476 17. Breiman L (2001) Random forests. *Machine Learning* 45:5-32.
- 477 18. Berk RA (2006) An introduction to ensemble methods for data  
478 analysis. *Socio Meth Res* 34:263-295.
- 479 19. Harland AD, Navarro JC, Davies PS, Fixter LM (1993) Lipids of some  
480 Caribbean and Red Sea corals - total lipid, wax esters, triglycerides  
481 and fatty acids. *Mar Biol* 117:113-117.
- 482 20. Carballeira NM, Sostre A, Ballantine, DL (1999) The fatty acid  
483 composition of tropical marine algae of the genus *Halimeda*  
484 (Chlorophyta). *Bot Mar* 42:383-387.
- 485 21. Tchernov D, et al. (2004) Membrane lipids of symbiotic algae are  
486 diagnostic of sensitivity to thermal bleaching in corals. *Proc Natl Acad*  
487 *Sci* 101:13531-13535.
- 488 22. Mashaghi A, et al. (2012) Hydration strongly affects the molecular and  
489 electronic structure of membrane phospholipids. *J Chem Phys*  
490 136(11):114709.
- 491 23. DeBerardinis RJ, Thompson CB (2012) Cellular Metabolism and  
492 Disease: What Do Metabolic Outliers Teach Us? *Cell* 148:1132-1144.
- 493 24. Bouslimani A, et al. (2015) Molecular cartography of the human skin  
494 surface in 3D. *Proc Natl Acad Sci* 112: E2120-E2129.

- 495 25. Petras D, et al. (2016) Mass Spectrometry-Based Visualization of  
496 Molecules Associated with Human Habitats. *Analyt Chem* 88:10775-  
497 10784.
- 498 26. Floros DJ, Petras D, Kaponi CA, Melnik AV, Ling TJ, Knight R,  
499 Dorrestein PC (2017). Mass spectrometry based molecular 3D-  
500 cartography of plant metabolites. *Front Plant Sci* 8:429.
- 501 27. Liaw A, Wiener M (2002) Classification and Regression by  
502 randomForest. *R News* 2:18-22.
- 503 28. Archer F (2016) rfPermute: Estimate Permutation p-Values for  
504 Random Forest Importance Metrics. R package version 2.1.1.  
505 Zenodo. <http://doi.org/10.5281/zenodo.60414>.  
506  
507

508 **Figure Captions**

509 **Figure 1. Data processing and generation based on a simplified molecular**

510 **network and two redundant mass shifts.** (A) GNPS used MS/MS

511 fragmentation spectra to elucidate molecular similarities and network similar

512 molecules (i.e. related molecules). (B) Redundant mass shifts between related

513 molecules were identified and annotated to known chemical groups when

514 possible. (C) Molecular features that differed by a redundant mass shift were

515 quantified based on MS. Data were generated for (D) the number of times each

516 redundant mass shift was observed across all networks, (E) the summed

517 abundance of all molecules exhibiting each redundant mass shift, and (F) the

518 sum of the differences in abundances between the more massive and less

519 massive molecules for all pairs of molecules connected by a mass shift.

520

521 **Figure 2. Molecular network of the coral MS/MS dataset.** (A) The global

522 molecular networks of MS/MS spectra from the coral reef holobiont metabolomic

523 dataset. Each node represents a unique or set of identical spectra (i.e., molecular

524 feature). Lines connecting the nodes represent their spectral similarity, creating

525 subnetworks that can be considered to be molecular families. Circles indicate

526 zoomed-in regions of selected subnetworks shown in (B). Node labels represent

527 parent masses and the line labels between the connected nodes represents the

528 mass shift between related molecular features. Nodes with diamond shapes had

529 a spectrum library match, (e.g., Lyso-PAF, as identified by Quinn et al. 2016; 12)

530 and are further labeled with the molecular names. The size of the nodes  
531 indicates the sample frequency in which the spectra were found.

532

533 **Figure 3. Results of tests measuring the extent to which holobionts were**

534 **resolved by MeMSSchem profiling.** (A) A visualization of the first two

535 dimensions of a Random Forests proximity matrix of the number of times that

536 each redundant mass shift was identified (counts data). The color of the filled

537 circle represents the holobiont type of the sample while the color of the halo

538 around each circle corresponds to the holobiont type it was placed in by the

539 Random Forests model (i.e., if the circle and halo are different colors the model

540 incorrectly categorized the sample). (B) An analogous representation of (A) for

541 the summed abundances of molecules grouped by the mass shifts they exhibit

542 among only the molecular features present in all holobionts. (C) An analogous

543 representation of (A) using the difference in abundances of molecules ‘gaining’

544 minus ‘losing’ a mass, summed by the mass shift they exhibit among only the

545 molecular features present in all holobionts. (D) An analogous representation of

546 (A) using the difference in abundances of molecules ‘gaining’ minus ‘losing’ a

547 mass, summed by the mass shift they exhibit among all the molecules in the

548 dataset. (E) A histogram of the permutation test from randomly generated

549 datasets to determine how well MeMSSchem profiling resolves each holobiont

550 type based on the model error. Letters above each line correspond to the model

551 error of the actual data in the figure panel matching that letter. The histograms

552 reflect the model errors of 1000 permutations of the actual data in which pairs  
553 were randomly binned while keeping the original proportions consistent. This was  
554 repeated for the data in (A–D), the distributions for which are shown in order  
555 and darkening color of counts, summed abundances, differences in abundances  
556 in molecules present in all holobionts, and differences in abundances in the  
557 entire molecular dataset.

558

559 **Figure 4. The annotated mass shifts that best differentiated each holobiont**  
560 **type.** (A) The annotated mass shifts that best distinguish between coral genera  
561 based on the mean decrease accuracy of a supervised Random Forests. (B) The  
562 annotated mass shifts that best distinguish between the non-coral holobiont  
563 types. (C) The annotated mass shifts that best distinguish the coral holobionts  
564 from the non-coral holobionts.

565

566

567

568

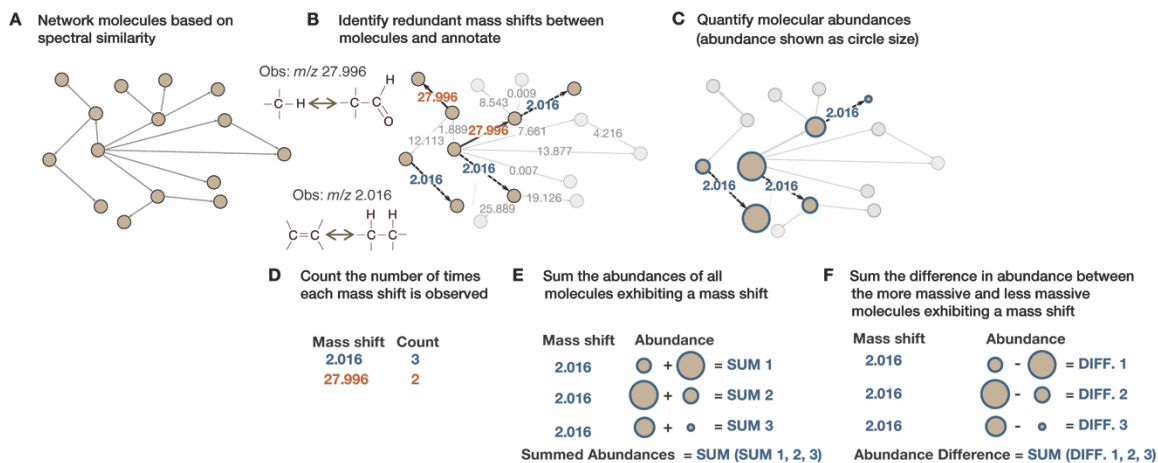
569

570

571

572

573



574

575

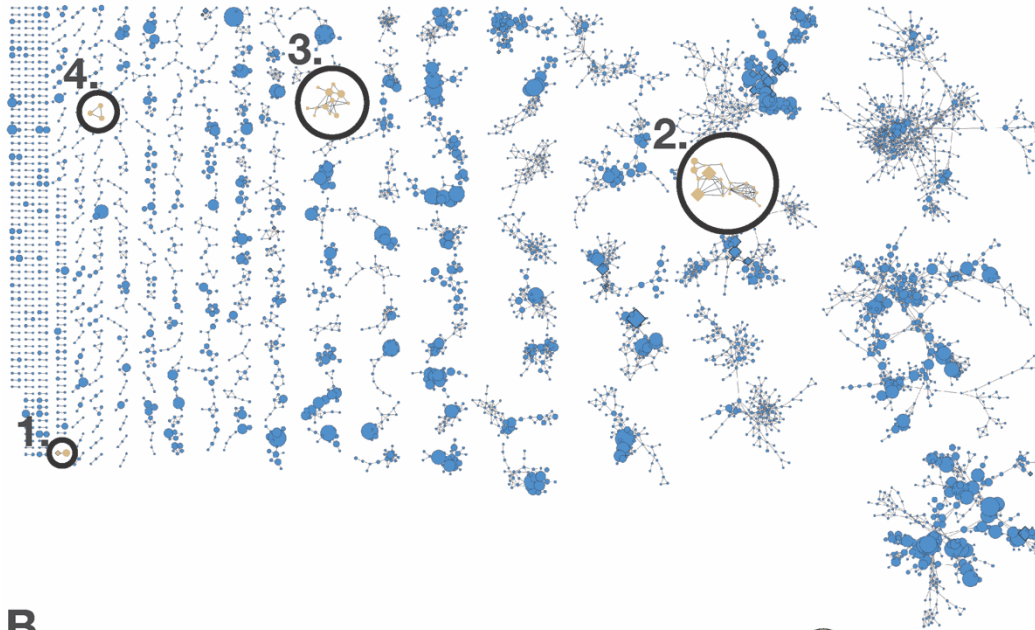
576 Fig. 1

577

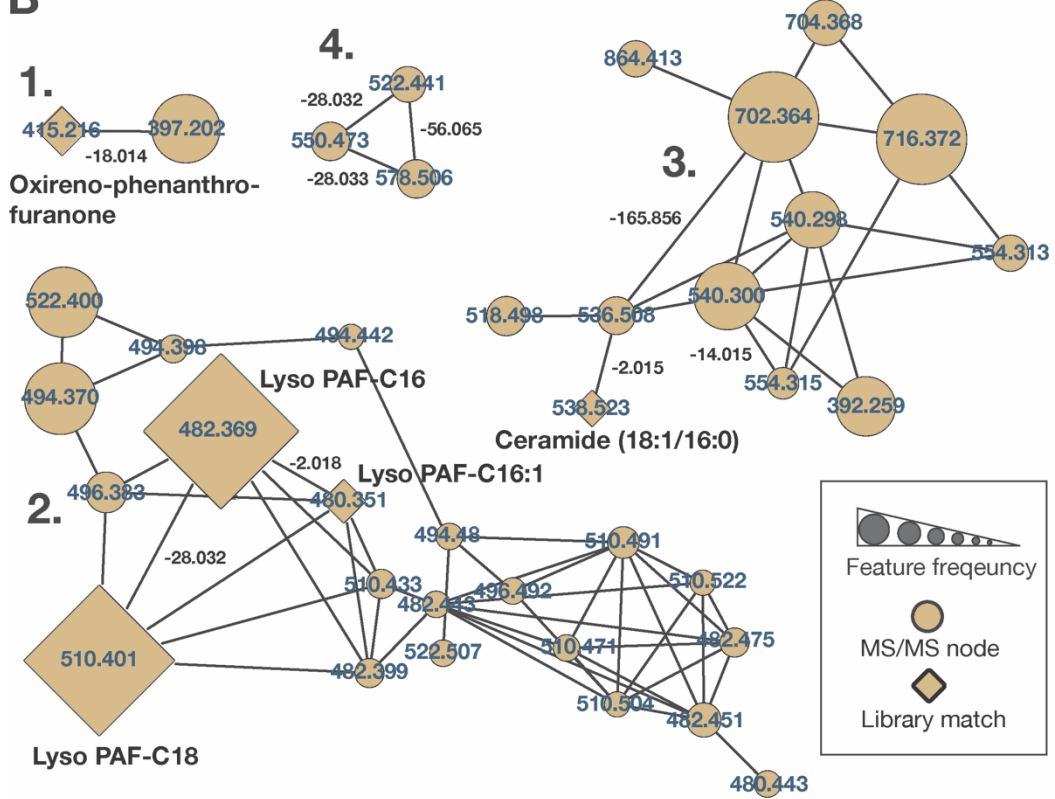
578

579

A

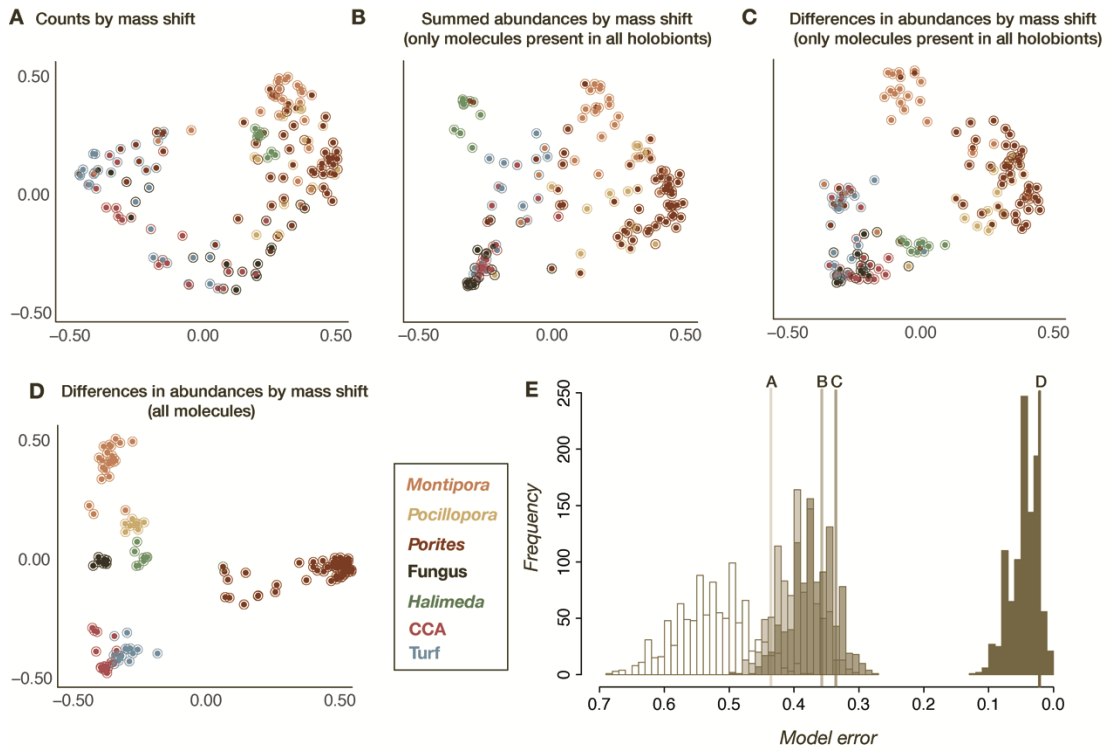


B



580  
581  
582  
583  
584

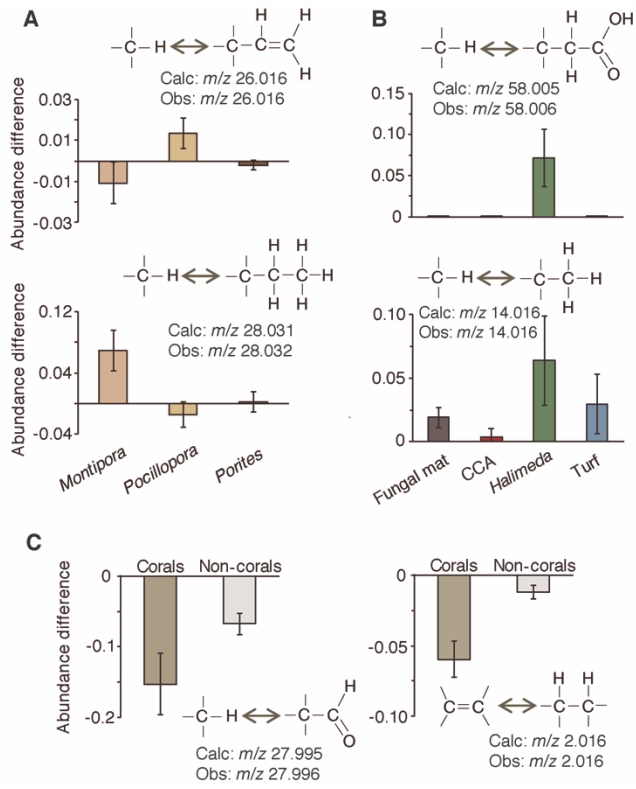
Fig. 2



585  
 586  
 587  
 588  
 589

Fig. 3





590

591

592

Fig. 4